RSC Advances

ROYAL SOCIETY OF CHEMISTRY

www.rsc.org/advances

RSC Advances

RSCPublishing

Communications

Near-infrared electrochemiluminescence from $Au_{25}(SC_2H_4Ph)_{18}^+$ clusters co-reacted with tri-*n*-propylamine

Cite this: DOI: 10.1039/x0xx00000x

Mahdi Hesari, Mark S. Workentin* and Zhifeng Ding*

Received ooth January 2012,
Accepted ooth January 2012

DOI: 10.1039/x0xx00000x

www.rsc.org/

The oxidation of $Au_{25}(SC_2H_4Ph)_{18}^+C_6F_5CO_2^-$ clusters along with tri-*n*-propylamine (TPrA) as a co-reactant produces very strong near-infrared electrochemiluminescence with emission peak wavelengths (872 and 945 nm) and intensities depending on the TPrA concentration and working electrode potential.

The $Au_{25}(SR)_{18}^z$ cluster family (Au_{25}^z, z =1–, 0 and 1+) has been shown to possess a number of interesting optical[1, 2] and electrochemical[3] properties that are dependent on the charge states. This should be very interesting and useful in electrochemiluminescence (ECL).[4-7] Near-infrared (NIR) ECL of Au_{25} clusters can be observed from electron transfer (ET) between electrogenerated radicals,[8] which might find great applications in desired *in vivo* bio-imaging.[9, 10] Recently, we examined the ECL of the Au_{25}^+ through annihilation of electrogenerated Au_{25}^{2+} and Au_{25}^{2-} species. The result showed very weak ECL similar to that of *visible* ECL of Au_{25}^- clusters in aqueous solution,[11, 12] most likely due to their short lifetime within the experiment time scale.[8] Furthermore, enhanced ECL originated from Au_{25}^{-*} upon relaxation to its ground state was observed in the benzoyl peroxide (BPO) co-reactant system, where Au_{25}^{2-} reacted with the benzoate radical (a strong oxidizing agent with E° > +1.5 V *vs*. SCE)[13] generated *via* the reduction of both Au_{25}^+ and BPO. To further explore and elucidate possible ECL emissive states and mechanisms, the system of Au_{25}^+ clusters in the presence of tri-*n*-propylamine (TPrA) should be very interesting. A number of Au_{25} oxidation states including Au_{25}^{2+}, Au_{25}^+, Au_{25}^0, Au_{25}^- and Au_{25}^{2-} can be easily accessed and a highly reducing TPrA radical ($TPrA^\bullet$, E°= -1.7 V *vs*. SCE)[14] can be generated by quickly deprotonating the intermediate, $TPrA^{+\bullet}$ after the oxidation of TPrA. Multiple excited states such as Au_{25}^{+*}, Au_{25}^{0*} and Au_{25}^{-*} are anticipated to be produced by interactions of Au_{25}^{2+}, Au_{25}^+ and Au_{25}^0 along with $TPrA^\bullet$, respectively. Unlike BPO, TPrA is more compatible with both aqueous and organic solvents, a desirable feature for many applications.

Herein we report the ECL of the Au_{25}^+ and TPrA co-reactant system, where ECL was interrogated by changing the TPrA concentration, [TPrA], and applied potential at the working electrode. We employed our newly developed spooling ECL spectroscopy to correlate the ECL spectra with the applied potential. As a result, we were able to elucidate ECL mechanisms and assign the excited states of the Au_{25} responsible for the observed ECL, namely Au_{25}^{+*}, Au_{25}^{0*} and Au_{25}^{-*}. Importantly, ECL intensity in the TPrA co-reactant system was 14 times higher than that observed that with BPO, due in part to the reduction power $TPrA^\bullet$.[15]

The pure Au_{25}^+ was prepared and characterized following published protocol (see ESI for detailed procedures and data).[8] The ECL studies were conducted using equipment described elsewhere.[8] While relevant electrochemistry of the Au_{25}^+ has been discussed recently,[8] it is important to keep in mind the two formal redox potentials, $E^\circ'(Au_{25}^+/Au_{25}^0)$= 0.185 V and $E^\circ'(Au_{25}^{2+}/Au_{25}^+)$= 0.817 V *vs.* SCE (see Fig. S3 in ESI). In a typical ECL experiment, a 0.1 mM solution of the Au_{25}^+ was prepared in 1:1 acetonitrile: benzene mixture containing 0.1 M tetra-*n*-butylammonium perchlorate (TBAP) as the supporting electrolyte in a glovebox using airtight cylindrical glass cell with a flat Pyrex window at the bottom for the ECL detection. To this solution a specific concentration of TPrA was added under Ar atmosphere blanket; the [TPrA] was varied from 6.3, to 12.5, 25, 50, 100, and 200 mM in order to gain insight into mechanistic details on the excited states responsible for the ECL emissions observed upon oxidation of both TPrA and Au_{25}^+.

Fig. S4 in the ESI shows the cyclic voltammogram (CV) and ECL-voltage curve of a 0.1 mM Au_{25}^+ electrolyte solution with 50 mM TPrA at a scan rate of 100 mVs^{-1}. The CV (black in Fig. S4A) demonstrates the dominating irreversible oxidation of TPrA to $TPrA^{\bullet+}$ with a peak potential of 0.880 V vs. SCE (eq. 1). The $TPrA^{\bullet+}$ intermediate deprotonates rapidly forming $TPrA^\bullet$ (eq. 2). The red curve in Fig. S4B is the corresponding ECL-voltage curve, illustrating the ECL intensity as a function of applied potential. The onset of ECL occurred at 0.643 V, a potential at which the electrogenerated $TPrA^\bullet$ reacted with Au_{25}^+ in the bulk solution and produced ECL light from the formed Au_{25}^{0*} excited state (eqs. 3-4).

$$T\Pr A \rightarrow T\Pr A^{\bullet+} + e \quad (1)$$

$$T\Pr A^{\bullet+} \rightarrow T\Pr A^{\bullet} + H^+ \quad (2)$$

$$Au_{25}^+ + T\Pr A^{\bullet} \rightarrow Au_{25}^{0*} + T\Pr A^+ \quad (3)$$

$$Au_{25}^{0*} \rightarrow Au_{25}^0 + h\nu_1 \quad (4)$$

Fig. 1 demonstrates the spooling ECL spectra acquired at a time interval of 1 s or a potential interval of 100 mV for the above solution during a cycle of the potential scanning between -0.557 and 1.142 V at a scan rate of 100 mVs^{-1}. The onset ECL

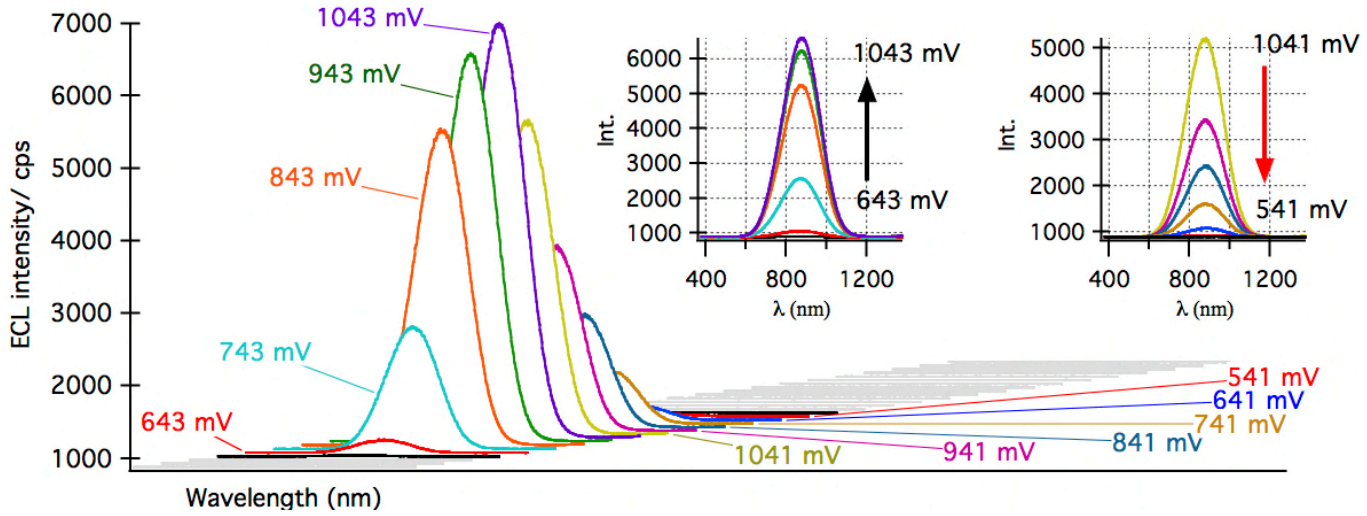

Figure 1. Spooling ECL spectra of 0.1 mM of Au_{25}^{+} with 50 mM TPrA during the potential scanning between -0.557 and 1.142 V at a scan rate of 100 mVs^{-1}. Insets present stack spectra showing ECL evolution and devolution.

spectrum was also at 0.643 V, which is identical to that from the ECL-voltage curve in Fig. S4B. The onset peak wavelength reads 872 nm in Fig. 1. The measured photoluminescence (PL) spectrum of electrogenerated Au_{25}° shown in Fig. S5 confirms that the PL emission at 865 nm belongs to the Au_{25}° excited state. The slight difference between the ECL and PL wavelengths is due to the self-absorption (inner-filter effect).[16] The ECL peak wavelength remained the same when the potential was scanned towards more positive potentials. At 0.743 V, for instance, the intensity augmented due to the increasing [TPrA$^{\bullet}$]. This is an indication of the same excited state generated via electron transfer from TPrA$^{\bullet}$ (E°= -1.7 eV)[15] to the LUMO of Au_{25}^{+} (eqs. 3-4). Possible electron transfer to the Au_{25}^{+} HOMO would not lead to any excited state. Also, at these potentials the Au_{25}° formed would be re-oxidized to Au_{25}^{+} leading to the electrocatalytic process for ECL.[17] At potentials more positive than 0.847 V (larger than $E^{\circ\prime}(Au_{25}^{2+}/Au_{25}^{+})$, 0.817 V), at which Au_{25}^{2+} was generated in the vicinity of the working electrode. Au_{25}^{+}* was expected to be produced via interaction of Au_{25}^{2+} with TPrA$^{\bullet}$(eqs. 5-6). The same peak wavelength of 872 nm was observed, Fig. 1. In contrast, the ECL intensity was increased dramatically. These agree well with the observations from the *in-situ* PL spectroscopy of the three species generated via thin layer electrolysis in the same electrolyte solution (Fig. S5 in ESI). The PL lead to the conclusion that Au_{25}°* and Au_{25}^{+}* have almost an identical emission peak wavelength (865 and 860 nm, respectively) but Au_{25}^{+}* has stronger emission light intensity. The above results validated our ECL reaction mechanism for the Au_{25}^{+}* generation and then light emission, eqs. 5-6. The ECL intensity at 0.847, 0.947 and 1.047 increased to 27, 34 and 36 times of that at 0.643 V. Not only was the Au_{25}^{+}* a stronger emitter than the Au_{25}°* but also the oxidation of TPrA (with a peak potential of 0.880 V) was centred in this potential region, leading to a high [TPrA$^{\bullet}$]. The combination of the two factors brought an ECL enhancement. The ECL peak intensity dropped gradually upon potential scanning to a little further positive potential (1.142 V) and back to 0.541 V. The depletion of the [TPrA$^{\bullet}$] caused a decrease in [Au_{25}^{+}*] or a switch to Au_{25}°*, and therefore a diminishing light emission. The ECL devolution can be clearly seen in the right inset in Fig. 1. The spooling ECL spectra give more information than ECL-voltage curve, Fig. S4.

$$Au_{25}^{2+} + T\,\mathrm{Pr}\,A^{\bullet} \rightarrow Au_{25}^{+*} + T\,\mathrm{Pr}\,A^{+} \qquad (5)$$

$$Au_{25}^{+*} \rightarrow Au_{25}^{+} + + h\nu_2 \qquad (6)$$

Fig. 2 shows the spooling ECL spectra of Au_{25}^{+} (0.1 mM) in the presence of 100 mM TPrA in a very similar potential region. The increased [TPrA] promoted a very high local [TPrA$^{\bullet}$] in the vicinity of the working electrode biased with an anodic potential. The onset ECL with 100 mM TPrA was delayed for 100 mV relative to that with 50 mM TPrA, which might be caused by the quenching of excited state by TPrA. This is a phenomena also observed with $Ru(bpy)_3^{2+}$ and other co-reactant systems.[14] More importantly, the ECL peak wavelength showed a pronounced red shift to 945 nm, Fig. 2, which was maintained the same in the ECL evolution and devolution as illustrated by the recorded spooling ECL spectra. Again, the PL spectrum of Au_{25}^{-} produced via electrolysis shows a peak wavelength at 945 nm with similar PL intensity to that of Au_{25}°, Fig. S5 in ESI. This means that Au_{25}^{-}* species can be differentiated by the longer peak wavelength from Au_{25}°* and Au_{25}^{+}*. Our PL results agree well with those reported by Kaufmann and Jin et al. upon electrolysis of Au_{25}^{-}.[18, 19] With the increased [TPrA$^{\bullet}$], it is plausible that ECL in Fig. 2 is due to the formation of Au_{25}^{-}* that emitted light upon relaxation to its ground state. The strong reducing agent, TPrA$^{\bullet}$ must act as an electron carrier to drive reduction reactions of Au_{25}^{+} (in the bulk at the ECL onset potential) and Au_{25}^{2+} (generated at the electrode biased with more positive potentials) to Au_{25}°, and all the way to Au_{25}^{2-} (eqs. 7-9). Au_{25}^{-}* was formed either via electron transfer from TPrA$^{\bullet}$ to the Au_{25}° LUMO (eq. 10) or that from Au_{25}^{2-} HOMO to Au_{25}° HOMO (eq. 11). Au_{25}^{-}* then relaxed to the ground state, emitting at the peak wavelength of 945 nm (eq. 12). It is interesting to notice that the ECL intensity measured in the unit of counts per second (cps) with 100 mM [TPrA] (Fig. 2) were lower than those with 50 mM [TPrA] (Fig. 2) because of the low luminescence efficiency of Au_{25}^{-}* relative to those of Au_{25}^{+}* and Au_{25}°* (Fig. S5), and the quenching of the excited state mentioned above.

When 200 mM TPrA was added to the system, the spooling ECL spectra showed the same unique peak wavelength at 945 nm (Fig. S6) and further reduced ECL intensity relative to that with 100 mM TPrA.

The Au_{25}^{+} cluster solution with TPrA concentrations of 6.3, 12.5 and 25 mM displayed a gradual increase in ECL intensity, which can be clearly seen from the corresponding accumulated ECL spectra recorded during 2 cycles of potential scanning, Fig. S7. The same peak wavelength at 875 nm as that with 50 mM TPrA was observed in the ECL evolution and devolution processes, featuring emissions from Au_{25}°* and Au_{25}^{+}* (see Figs. S8-10 in ESI). The accumulated ECL spectra revealed the same changing pattern of the ECL peak

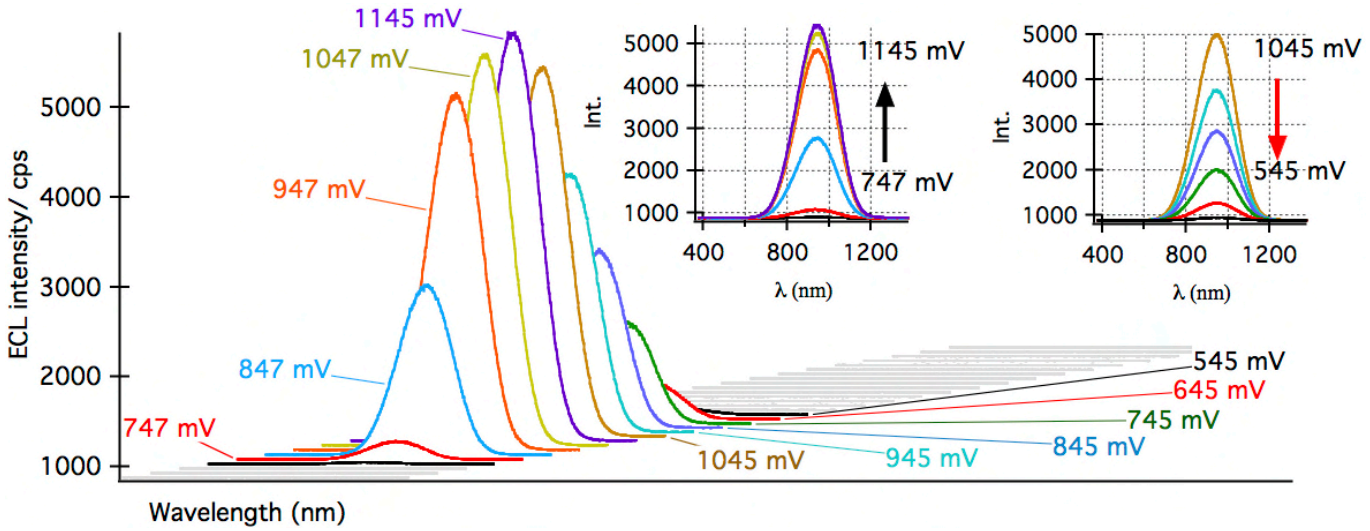

Figure 2. Spooling ECL spectra of 0.1 mM of Au_{25}^{+} with 100 mM TPrA during the potential scanning between -0.554 and 1.146 V at a scan rate of 100 mVs^{-1}. Insets represent stack spectra demonstrating ECL evolution and devolution.

wavelength vs TPrA concentration as in the spooling ECL spectroscopy: ECL is attributed to the Au_{25}^{+}* and Au_{25}^{0}* in the presence of [TPrA] less than 50 mM, while the light emission is mainly from Au_{25}^{-}* upon further increase in [TPrA].

$$Au_{25}^{+} + TPrA^{\bullet} \rightarrow Au_{25}^{0} + TPrA^{+} \quad (7)$$

$$Au_{25}^{0} + TPrA^{\bullet} \rightarrow Au_{25}^{-} + TPrA^{+} \quad (8)$$

$$Au_{25}^{-} + TPrA^{\bullet} \rightarrow Au_{25}^{2-} + TPrA^{+} \quad (9)$$

$$Au_{25}^{0} + TPrA^{\bullet} \rightarrow Au_{25}^{-*} + TPrA^{+} \quad (10)$$

$$Au_{25}^{2-} + Au_{25}^{0} \rightarrow Au_{25}^{-*} + Au_{25}^{-} \quad (11)$$

$$Au_{25}^{-*} \rightarrow Au_{25}^{-} + h\nu_3 \quad (12)$$

The relative ECL quantum yield (Φ) was calculated for each TPrA concentration in reference to that of $Ru(bpy)_3^{2+}$ /TPrA system (see Table S1). For example, in the presence of 25 mM TPrA a relative efficiency as high as 116% was reached. Please also note that with high [TPrA], the ECL quenching in the $Ru(bpy)_3^{2+}$/TPrA co-reactant system is more dramatic than that in the Au_{25}^{+}/TPrA one.[14] That is the reason why the relative efficiency in Table S1 shows a very high efficiency with [TPrA] larger than 100 mM.

Conclusions

NIR ECL in the Au_{25}^{+} /TPrA co-reactant system was found to be stronger than that of the Au_{25}^{+}/BPO system. The spooling ECL spectroscopy of the Au_{25}^{+}/TPrA co-reactant system was able to unambiguously discriminate three excited states, Au_{25}^{0}*, Au_{25}^{+}* and Au_{25}^{-}*, and elucidate the corresponding generation mechanisms by means ECL peak wavelengths and intensity. It was discovered that TPrA concentration played a very important role in electrogenerated light emissions from the three species. It is plausible that NIR-ECL of Au_{25}^{+} clusters can be tuned by varying the TPrA concentration and applied potential. All these will be helpful for the ECL community and molecular electrochemists in general.

Notes and references

1 G. Wang, R. Guo, G. Kalyuzhny, J.-P. Choi and R. W. Murray, *J. Phys. Chem. B*, 2006, **110**, 20282-20289.
2 Z. Wu and R. Jin, *Nano Lett.*, 2010, **10**, 2568-2573.
3 D. Lee, R. L. Donkers, G. Wang, A. S. Harper and R. W. Murray, *J. Am. Chem. Soc.*, 2004, **126**, 6193-6199.
4 H. Qi, J. J. Teesdale, R. C. Pupillo, J. Rosenthal and A. J. Bard, *J. Am. Chem. Soc.*, 2013, **135**, 13558-13566.
5 F. Pinaud, L. Russo, S. Pinet, I. Gosse, V. Ravaine and N. Sojic, *J. Am. Chem. Soc.*, 2013, **135**, 5517-5520.
6 S. Parajuli and W. Miao, *Anal. Chem.*, 2013, **85**, 8008-8015.
7 A. J. Bard, *Electrogenerated Chemiluminescence*, Marcel Dekker, 2004.
8 K. N. Swanick, M. Hesari, M. S. Workentin and Z. Ding, *J. Am. Chem. Soc.*, 2012, **134**, 15205-15208.
9 V. W. K. Ng, R. Berti, F. Lesage and A. Kakkar, *J. Mater. Chem. B*, 2013, **1**, 9-25.
10 R. Weissleder, *Nat. Biotech.*, 2001, **19**, 316-317.
11 L. Li, H. Liu, Y. Shen, J. Zhang and J.-J. Zhu, *Anal. Chem.*, 2011, **83**, 661-665.
12 Y.-M. Fang, J. Song, J. Li, Y.-W. Wang, H.-H. Yang, J.-J. Sun and G.-N. Chen, *Chem. Commun.*, 2011, **47**, 2369.
13 E. A. Chandross and F. I. Sonntag, *J. Am. Chem. Soc.*, 1966, **88**, 1089-1096.
14 R. Y. Lai and A. J. Bard, *J. Phys. Chem. A*, 2003, **107**, 3335-3340.
15 R. Y. Lai, J. J. Fleming, B. L. Merner, R. J. Vermeij, G. J. Bodwell and A. J. Bard, *J. Phys. Chem. A*, 2004, **108**, 376-383.
16 A. B. Nepomnyashchii, M. Broering, J. Ahrens, R. Krueger and A. J. Bard, *J. Phys. Chem. C*, 2010, **114**, 14453-14460.
17 W. Miao, J. Choi and A. Bard, *J. Am. Chem. Soc.*, 2002, **124**, 14478-14485.
18 D. R. Kauffman, D. Alfonso, C. Matranga, G. Li and R. Jin, *J. Phys. Chem. Lett.*, 2012, **4**, 195-202.
19 D. R. Kauffman, D. Alfonso, C. Matranga, H. Qian and R. Jin, *J. Am. Chem. Soc.*, 2012, **134**, 10237-10243.

Department of Chemistry and Centre for Advanced Materials and Biomaterials Research, The University of Western Ontario, 1151 Richmond St., London, ON, CANADA N6A 5B7. Fax: +1519 661 2166; Tel: +1 519 661 2111 ext 86161; E-mail: zfding@uwo.ca

† Electronic Supplementary Information (ESI) available: $Au_{25}(SC_2H_4Ph)_{18}^{+}$ synthesis and characterization (^{1}HNMR and Uv-Vis-NIR spectra), Au_{25}^{+} cyclic voltammogram along with the ECL-voltage curve, photoluminescence of electrogenerated Au_{25}^{z} (z= +1, 0 and 1-) species, supplementary spooling ECL spectra, and tabled ECL efficiencies. See DOI: 10.1039/b000000x/